

The scaling and universality of conventional and inverse magnetocaloric effects in Heusler alloys

Anis Biswas, T. L. Phan, N. H. Dan, P. Zhang, S. C. Yu et al.

Citation: [Appl. Phys. Lett.](#) **103**, 162410 (2013); doi: 10.1063/1.4825166

View online: <http://dx.doi.org/10.1063/1.4825166>

View Table of Contents: <http://apl.aip.org/resource/1/APPLAB/v103/i16>

Published by the [AIP Publishing LLC](#).

Additional information on Appl. Phys. Lett.

Journal Homepage: <http://apl.aip.org/>

Journal Information: http://apl.aip.org/about/about_the_journal

Top downloads: http://apl.aip.org/features/most_downloaded

Information for Authors: <http://apl.aip.org/authors>



Re-register for Table of Content Alerts

Create a profile.



Sign up today!



The scaling and universality of conventional and inverse magnetocaloric effects in Heusler alloys

Anis Biswas,^{1,a)} T. L. Phan,² N. H. Dan,³ P. Zhang,² S. C. Yu,^{2,a)} H. Srikanth,^{1,a)} and M. H. Phan^{1,a)}

¹Department of Physics, University of South Florida, Tampa, Florida 33620, USA

²Department of Physics, Chungbuk National University, 361-763 Cheongju, South Korea

³Institute of Materials Science, Vietnam Academy of Science and Technology, Cau Giay, Hanoi, Vietnam

(Received 25 June 2013; accepted 27 September 2013; published online 17 October 2013)

We report a comparative study of the universal behaviors of conventional and inverse magnetocaloric effects (CMCE and IMCE, respectively) that coexist in Heusler alloys of $\text{Ni}_{50}\text{Mn}_{50-x}\text{Sn}_x$ ($x \sim 13, 14$) and $\text{Ni}_{50-x}\text{Pr}_x\text{Mn}_{37}\text{Sn}_{13}$ ($x \sim 1, 3$). In contrast to CMCE associated with a first-order phase transition (FOPT), we show that it is possible to construct a universal master curve to describe the temperature dependence of magnetic entropy change $\Delta S_M(T)$ in different applied fields without rescaling the temperature axis for IMCE associated with FOPT. This universal behavior is shown to be different from that observed for CMCE associated with a second-order phase transition. The proposed universal curves provide an effective method of extrapolating ΔS_M of materials associated with CMCE and IMCE in any range of temperatures and magnetic fields, giving useful guidance on the development of active magnetic refrigerants.

© 2013 AIP Publishing LLC. [<http://dx.doi.org/10.1063/1.4825166>]

Magnetic refrigeration based on the magnetocaloric effect (MCE) has emerged as an attractive option in the generation of energy-efficient cooling technologies.¹⁻⁴ Given its higher cooling efficiency, environmental friendliness, and compactness, this technology has potential to replace existing gas compression cycle based refrigeration techniques.^{2,4} The majority of research in this area is to develop materials that are cost-effective and exhibit large MCE (large isothermal magnetic entropy change ΔS_M or large adiabatic temperature change ΔT_{ad}) over a wide temperature range. To fully exploit the MCE of a given material, it is essential to understand how ΔS_M or ΔT_{ad} evolves with temperature (T) and magnetic field (H). Therefore, methods for constructing universal curves to describe the temperature and magnetic field dependences of ΔS_M obtained for a variety of magnetocaloric materials have been proposed.⁵⁻¹³ Franco *et al.* have derived an excellent phenomenological rescaling procedure for both ΔS_M and ΔT_{ad} , which allows the extrapolation of these parameters in temperatures and magnetic fields, thus providing guidance on design and fabrication of magnetic refrigerants for use in actual cooling devices.⁴⁻⁶ It is worth noting that universal behavior manifested in the collapse of $\Delta S_M(T)$ curves after a scaling procedure has been established mostly for materials undergoing a second order phase transition (SOPT).^{4,8} The scaling features that underlie this behavior have been reported to break down (or collapse of the modified $\Delta S_M(T)$ curves fails) in case of materials with a first order phase transition (FOPT).⁸ As a result, whether or not collapse is achieved can be applied as a method of distinguishing SOPT from FOPT.¹³ However, a recent study has shown that $\Delta S_M(T)$ curves of FOPT materials, such as $\text{MnFeP}_{1-x}\text{As}_x$, can be collapsed on a universal master curve, leaving an open question regarding the underlying mechanism of the scaling and universality of

the MCE in FOPT materials.² While the universal behavior of $\Delta S_M(T)$ curves has been extensively studied in SOPT materials exhibiting *conventional* MCEs⁵⁻¹⁰ (e.g., the magnetic entropy decreases with an applied magnetic field), we have recently shown that it is also possible to construct a universal master curve to describe $\Delta S_M(T)$ in different applied fields for SOPT materials exhibiting *inverse* MCEs (e.g., the magnetic entropy increases with an applied magnetic field).^{11,12} Importantly, we find that in contrast to the case of conventional magnetocaloric effect (CMCE) materials, the universal master curve can be constructed in inverse magnetocaloric effect (IMCE) systems for different H without rescaling temperature axis. While our preliminary study was mainly focused on the IMCE behavior of antiferromagnetic SOPT manganites,¹¹ the observations of IMCE in some ferromagnetic FOPT systems, such as Heusler Ni-Mn-Sn alloys,¹⁴⁻¹⁷ raise a question regarding the validity of the universality of the IMCE in these systems. Since such IMCE materials are potentially important components in active magnetic refrigerators,¹⁴ it is vital to understand the temperature and field dependences of ΔS_M in these systems.

In this Letter, we report a comparative study of the scaling and universality of the conventional and inverse magnetocaloric effects that coexist in a single material system. A systematic analysis of these effects has been performed on Heusler alloys of $\text{Ni}_{50}\text{Mn}_{36}\text{Sn}_{14}$, $\text{Ni}_{50}\text{Mn}_{37}\text{Sn}_{13}$, $\text{Ni}_{49}\text{Pr}_1\text{Mn}_{37}\text{Sn}_{13}$, and $\text{Ni}_{47}\text{Pr}_3\text{Mn}_{37}\text{Sn}_{13}$. Doping concentration and elements were varied to examine the validity of the universality of the CMCE and IMCE. Our study shows that a universal curve of $\Delta S_M(T)$ exists for the case of IMCE associated with FOPT, which is similar to the case of antiferromagnetic SOPT materials but contrary to the case of CMCE systems. The proposed universal curve method allows one to extrapolate the magnetic entropy change and the relative cooling power in any temperature and magnetic field range, which is of practical importance in assessing

^{a)}Electronic addresses: anisbiswas@usf.edu; scyu@chungbuk.ac.kr; sharihar@usf.edu; and phanm@usf.edu.

the usefulness of magnetocaloric materials for active magnetic refrigeration technology.

A series of Heusler alloys including $\text{Ni}_{50}\text{Mn}_{36}\text{Sn}_{14}$ (No. 1), $\text{Ni}_{50}\text{Mn}_{37}\text{Sn}_{13}$ (No. 2), $\text{Ni}_{49}\text{Pr}_1\text{Mn}_{37}\text{Sn}_{13}$ (No. 3), and $\text{Ni}_{47}\text{Pr}_3\text{Mn}_{37}\text{Sn}_{13}$ (No. 4) that we have studied in this work were prepared by melt-spinning and arc-melting methods from high-purity Ni, Mn, Sn, and Pr powders. The ratio of Mn/Sn was varied and partial substitution of Pr for Ni was chosen, to examine the doping effects on the universal behavior of both CMCE and IMCE in Heusler-type alloys. X-ray diffraction measurements and analysis were performed on all the prepared samples, which confirm the formation of single-phased polycrystalline materials. A commercial superconducting quantum interference device (SQUID) based magnetometer was used to investigate the magnetic and magnetocaloric properties of the samples.

The temperature dependence of susceptibility $\chi(T)$ for the samples was studied in both zero-field-cooled (ZFC) and field-cooled (FC) regimes in a field of 15 mT, and the results are shown in Fig. 1. As expected for this kind of materials, two distinct magnetic transitions are observed in $\chi(T)$ curves. On lowering temperature, a paramagnetic to ferromagnetic (PM–FM) transition in the austenitic phase occurs at high temperature (T_C^A), which is followed by a first order transition from the austenitic to martensitic state (A – M) at low temperature (T_{AM}).^{14–17} It has been reported that the A – M transition leads the alloys into a magnetic state of lower magnetization giving rise to a pronounced drop in the magnetization.^{14,16} In some cases, however, the magnetization in the martensitic state starts to increase sharply below a certain temperature, which is known as the martensitic Curie temperature (T_C^M).^{16,17} In the present case, values of T_C^A are determined to be about 310, 302, 297, and 303 K, while values of T_{AM} are \sim 165, 255, 225, and 230 K for Samples No. 1, No. 2, No. 3, and No. 4, respectively. Except for Sample No. 1, the other three samples exhibit the transition at T_C^M .

In order to evaluate the MCE in the present samples, the isothermal magnetization curves of the samples were

measured with a field step of 0.05 mT in a range of 0–4 T and a temperature interval of 3 K in a range of temperatures around T_C^A and T_{AM} . From these M – H isotherms (for clarity, some representative M – H curves are shown in the insets of Fig. 2), the magnetic entropy change (ΔS_M) of the samples has been calculated using the Maxwell relation,²

$$\Delta S_M = \mu_0 \int_0^{H_{\max}} \left(\frac{\partial M}{\partial T} \right)_H dH, \quad (1)$$

where M is the magnetization, H is the magnetic field, and T is the temperature. Figure 2 shows the temperature dependence of $-\Delta S_M$ for different magnetic field changes up to 4 T for all samples investigated. As expected, the samples exhibit large magnetic entropy changes around the T_C^A and T_{AM} , corresponding to the CMCE and IMCE. While the increase of Mn/Sn ratio was found to increase the IMCE and retain the CMCE in $\text{Ni}_{50}\text{Mn}_{50-x}\text{Sn}_x$, the substitution of Pr for Ni decreased both the IMCE and CMCE in $\text{Ni}_{50-x}\text{Pr}_x\text{Mn}_{37}\text{Sn}_{13}$. It is worth mentioning that the IMCEs of the Pr-containing samples were much smaller than those of the Pr-free samples. This indicated that the IMCE of $\text{Ni}_{50}\text{Mn}_{37}\text{Sn}_{13}$ was strongly suppressed by Pr doping into Ni sites. While the variation of Mn/Sn ratio and the substitution of Pr for Ni were observed to alter the austenitic PM–FM transition and the A – M transition and consequently the magnitude of their CMCE/IMCE, we show below these doping effects do not violate the universal behaviors of CMCE and IMCE.

In the present work, we investigated the magnetic field dependence of ΔS_M in the temperature ranges corresponding to IMCE and CMCE. It has been suggested that for magnetocaloric materials, ΔS_M follows a power law dependence of H :^{4,5}

$$\Delta S_M \sim H^n. \quad (2)$$

The exponent, n , can be precisely calculated using the following relation:

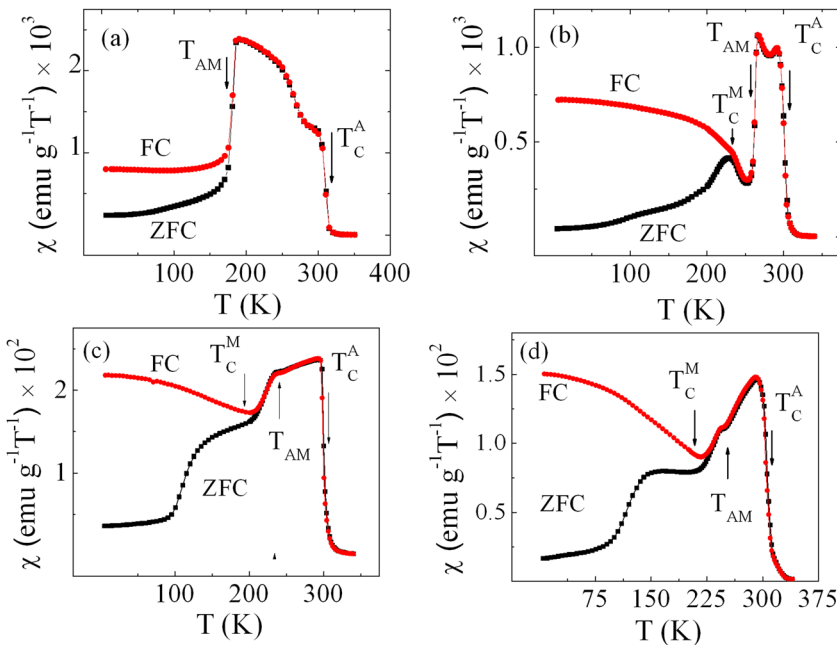


FIG. 1. Temperature dependence of susceptibility measured in zero-field-cooled and field-cooled regimes for (a) $\text{Ni}_{50}\text{Mn}_{36}\text{Sn}_{14}$, (b) $\text{Ni}_{50}\text{Mn}_{37}\text{Sn}_{13}$, (c) $\text{Ni}_{49}\text{Pr}_1\text{Mn}_{37}\text{Sn}_{13}$, and (d) $\text{Ni}_{47}\text{Pr}_3\text{Mn}_{37}\text{Sn}_{13}$. All the transitions are indicated by arrows.

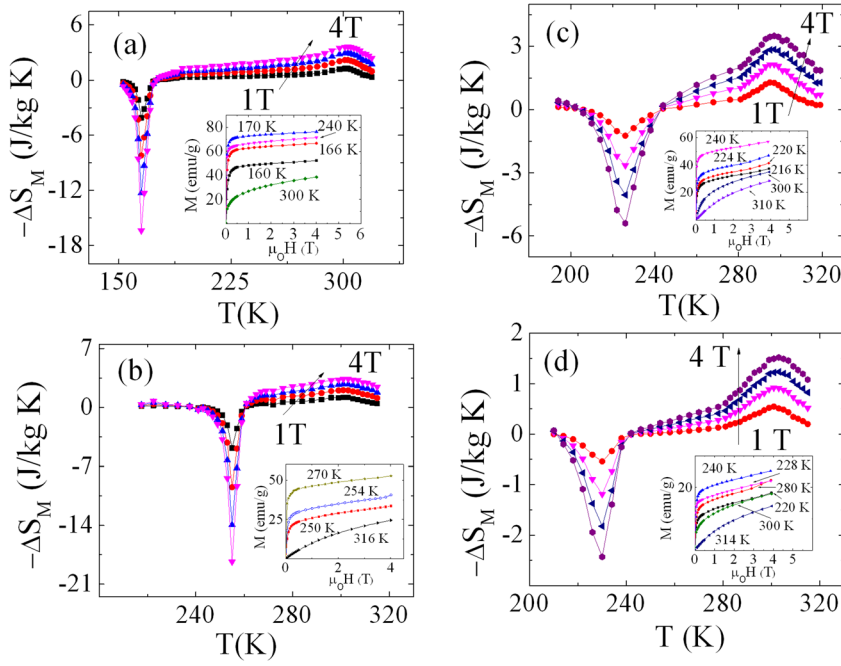


FIG. 2. Temperature dependence of $-\Delta S_M$ for different magnetic fields for (a) $\text{Ni}_{50}\text{Mn}_{36}\text{Sn}_{14}$; (b) $\text{Ni}_{50}\text{Mn}_{37}\text{Sn}_{13}$; (c) $\text{Ni}_{49}\text{Pr}_1\text{Mn}_{37}\text{Sn}_{13}$; (d) $\text{Ni}_{47}\text{Pr}_3\text{Mn}_{37}\text{Sn}_{13}$. Insets: representative $M(H)$ curves for the samples at selected temperatures.

$$n = \frac{d \ln |\Delta S_M|}{d \ln H} \quad (3)$$

Such a power law relation is valid for both cases of IMCE and CMCE for all samples investigated. As a representative

example, we show the linear $\ln |\Delta S_M|$ vs. $\ln H$ curves (indicating a power law dependence of ΔS_M) for $\text{Ni}_{50}\text{Mn}_{36}\text{Sn}_{14}$ (Sample No. 1) for IMCE (Fig. 3(a)) and CMCE (Fig. 3(b)). We find that for CMCE, n is dependent on both H and T (n shows a minimum around T_C^A , see, for example, in inset of

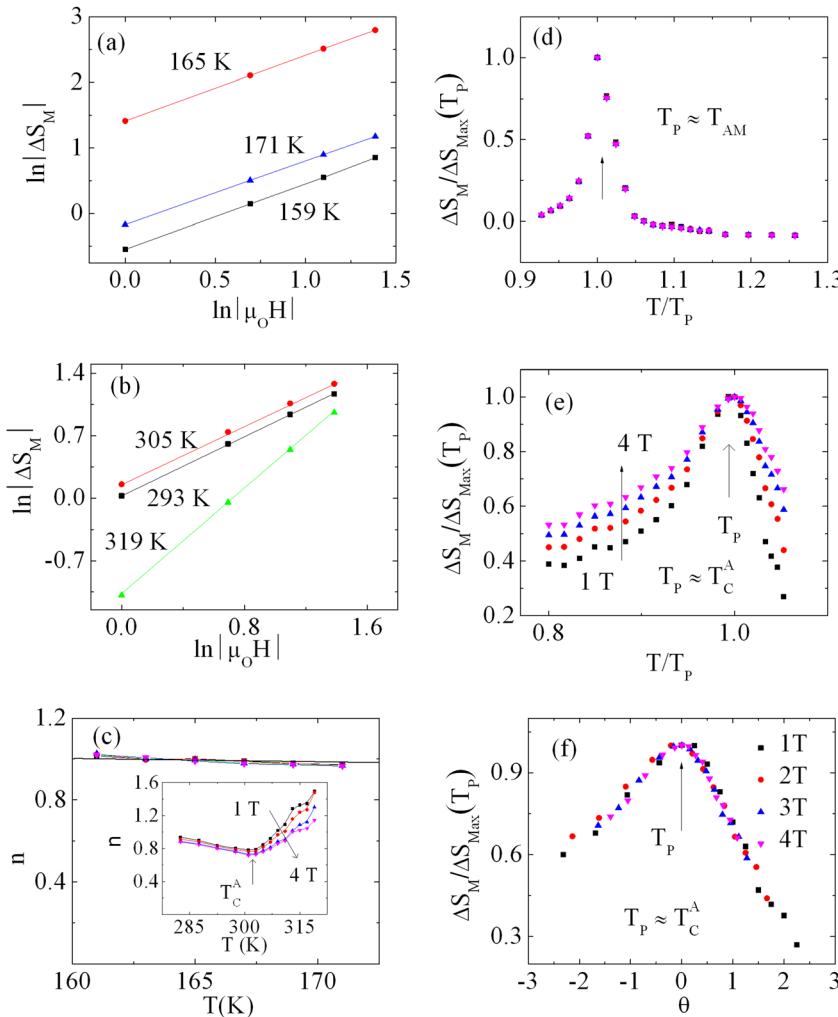


FIG. 3. (a) Linear $\ln |\Delta S_M|$ vs. $\ln H$ curves at three representative temperatures (below, above, and around T_{AM}) for $\text{Ni}_{50}\text{Mn}_{36}\text{Sn}_{14}$ (No. 1) indicating the power law dependence of ΔS_M with H ; (b) Linear $\ln |\Delta S_M|$ vs. $\ln H$ curves at three temperatures (below, above, and around T_C^A); (c) temperature dependence of n in different magnetic fields for Sample No. 1 in the temperature range corresponding to IMCE (Inset: n vs. T curves for different magnetic fields in the temperature region around T_C^A); (d) universal $\Delta S_M / \Delta S_{M, \text{max}}$ vs. T/T_p curve for the same sample ($T_p \approx T_{AM}$). The peak corresponding to IMCE is indicated by an arrow; (e) Failure of constructing a universal curve for $-\Delta S_M(T)$ associated with CMCE near T_C^A following the same protocol followed in case of IMCE for the sample; (f) The universal curve near T_C^A after rescaling the temperature axis according to Eq. (4).

Fig. 3(c)), as reported in previous works for other CMCE materials.^{5,6,8} In contrast to CMCE, however, n is *independent* of H and T for IMCE ($n \sim 1 \pm 0.12$ for $\text{Ni}_{50}\text{Mn}_{36}\text{Sn}_{14}$ and $\text{Ni}_{50}\text{Mn}_{37}\text{Sn}_{13}$; $n \sim 1.1 \pm 0.2$ for the Pr-containing samples) (Fig. 3(c)).

Since n is independent of H and T for IMCE, all $\Delta S_M(T)/\Delta S_{Max}$ vs. T/T_p curves obtained at different magnetic fields fall onto a single universal curve, where ΔS_{Max} is the peak value of $\Delta S_M(T)$ and T_p is the temperature corresponding to the peak ($T_p \sim T_{AM}$) for these alloys. It should be pointed out that the rescaling of temperature axis is not required to obtain such a universal curve in the IMCE case (see Fig. 3(d) and Figs. 4(a)–4(c)), while it is needed for the case of CMCE (see Figs. 3(e) and 3(f) and Figs. 4(d)–4(i)). It is clear that for CMCE the $\Delta S_M(T)/\Delta S_{Max}$ vs. T/T_p curves ($T_p = T_C^A$) did not collapse on a universal master curve (Fig. 3(e) and Figs. 4(d)–4(f)). The universal curve for the case of CMCE was only constructed when plotting $\Delta S_M(T)/\Delta S_{Max}$ against θ (Fig. 3(f) and Figs. 4(g)–4(i)), where θ is the temperature variable defined by

$$\theta = (T - T_C^A)/(T_r - T_C^A), \quad (4)$$

with T_r being a reference temperature corresponding to a certain fraction “ f ” that satisfies $\Delta S_M(T_r)/\Delta S_M(T_C^A) = f$.

It has been pointed out that uncertainty associated with the collapsing of $\Delta S_M(T)$ curves on to a universal curve should be quantified for each case.^{2,4,18} For this purpose, a parameter called dispersion (d) corresponding to each point in the universal curve is defined as⁴

$$d = 100 \times \frac{W}{(\Delta S_M/\Delta S_{Max})}. \quad (5)$$

In Eq. (5), “ W ” is the vertical shift of each entropy curve with respect to its mean value. The appearance of dispersion is related to the inherent uncertainty associated with the measurement procedure.¹⁸ For all samples investigated in the present work, the calculated value of d is less than 15%. This obtained value of d is within the range of that for different materials showing CMCE due to SOPT. However, it has been noted that d can be $\sim 100\%$ for CMCE due to FOPT, indicating the failure of construction of a universal curve for this case.^{11,12} In this context, our present results are very interesting as we show that the universal behavior of IMCE

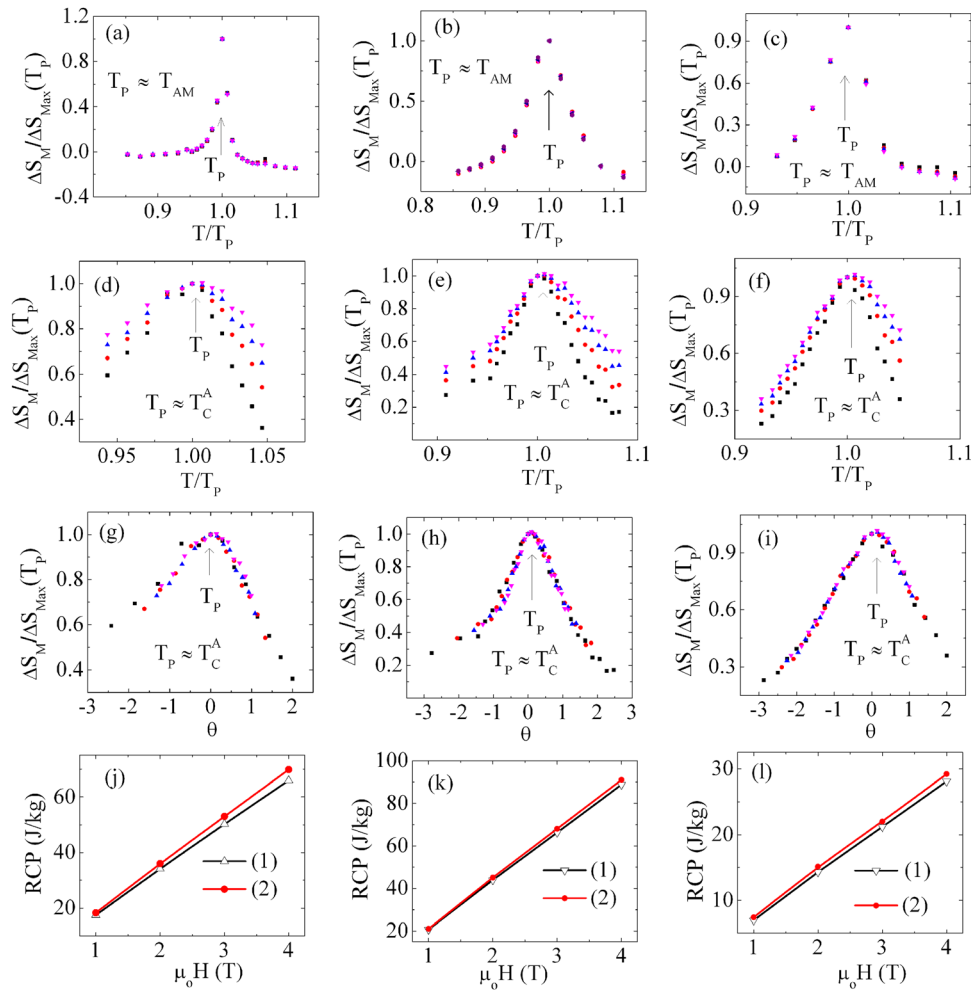


FIG. 4. All $\Delta S_M/\Delta S_{Max}$ vs. T/T_p (where, $T_p \approx T_{AM}$) curves for different fields fall onto a universal curve for (a) $\text{Ni}_{50}\text{Mn}_{37}\text{Sn}_{13}$; (b) $\text{Ni}_{49}\text{Pr}_1\text{Mn}_{37}\text{Sn}_{13}$; (c) $\text{Ni}_{47}\text{Pr}_3\text{Mn}_{37}\text{Sn}_{13}$. The peaks corresponding to IMCE are indicated by arrows. The failure of constructing a universal curve for CMCE around T_C^A without rescaling temperature axis for: (d) $\text{Ni}_{50}\text{Mn}_{37}\text{Sn}_{13}$, (e) $\text{Ni}_{49}\text{Pr}_1\text{Mn}_{37}\text{Sn}_{13}$, and (f) $\text{Ni}_{47}\text{Pr}_3\text{Mn}_{37}\text{Sn}_{13}$. The universal curve to describe $\Delta S_M(T)$ near that transition is constructed after rescaling the temperature axis using Eq. (4) for: (g) $\text{Ni}_{50}\text{Mn}_{37}\text{Sn}_{13}$, (h) $\text{Ni}_{49}\text{Pr}_1\text{Mn}_{37}\text{Sn}_{13}$, and (i) $\text{Ni}_{47}\text{Pr}_3\text{Mn}_{37}\text{Sn}_{13}$. The magnetic field dependence of RCP for the samples, calculated from (1) the temperature dependence of ΔS_M and (2) from the universal curve using Eq. (6): (j) $\text{Ni}_{50}\text{Mn}_{37}\text{Sn}_{13}$, (k) $\text{Ni}_{49}\text{Pr}_1\text{Mn}_{37}\text{Sn}_{13}$, (l) $\text{Ni}_{47}\text{Pr}_3\text{Mn}_{37}\text{Sn}_{13}$.

not only exists in materials associated with SOPT but also with FOPT.

One of the important figures of merit for magnetic refrigerants is relative cooling power (*RCP*).^{1,19,20} As *n* is independent of *H* and *T* for the samples in the temperature range associated with IMCE, *RCP* scales with *H*^{*n*} with the same value of *n*, defined in Eq. (3). As a result, it is possible to estimate *RCP* of an IMCE material in different magnetic fields from a universal curve, which is given by

$$RCP = (FWHM_{univ}) \times T_P \times \Delta S_{Max}, \quad (6)$$

where $FWHM_{univ}$ is the full width at half maximum of the universal curve. From the universal curves shown in Figs. 3 and 4, we calculated the *RCP* of samples for different values of *H* and found that the *RCP* values calculated from Eq. (6) are almost equal to those calculated from the experimental data. For example, a comparison between the magnetic field dependence of *RCP* and that calculated from the universal curve for Sample Nos. 2, 3, and 4 is shown in Figs. 4(j)–4(l). This proves that the proposed universal curves are a very useful method for predicting values of ΔS_M and *RCP* of IMCE materials in high magnetic field ranges with no need for performing actual experiments.

In summary, we have developed a simple method for constructing a universal curve to describe temperature dependence of magnetic entropy change and relative cooling power associated with the inverse magnetocaloric effect in Heusler-based alloys. This method allows one to extrapolate the magnetic entropy change and the relative cooling power in any range of temperatures and magnetic fields, giving a good guidance on the design of active magnetic refrigerant materials for use in magnetic cooling devices. We have also shown the difference in nature of the scaling and universality between the inverse magnetocaloric effect and the conventional magnetocaloric effect.

Research at USF was supported by DOE BES Physical Behavior of Materials Program through Grant Number DE-FG02-07ER46438 (Magnetic studies). Research at CBNU was supported by the Converging Research Center Program funded by the Ministry of Education, Science and Technology (2012K001431). M.H.P. acknowledges the support from FCASST.

- ¹K. A. Gschneidner, Jr., V. K. Pecharsky, and A. O. Tsokol, *Rep. Prog. Phys.* **68**, 1479 (2005).
- ²A. Smith, C. R. H. Bahl, R. Bjork, K. Engelbrecht, K. K. Nielsen, and N. Pryds, *Adv. Energy Mater.* **2**, 1288 (2012).
- ³K. G. Sandeman, *Scr. Mater.* **67**, 566 (2012).
- ⁴V. Franco, J. S. Blazquez, B. Ingale, and A. Conde, *Annu. Rev. Mater. Res.* **42**, 305 (2012).
- ⁵V. Franco, J. S. Blazquez, and A. Conde, *Appl. Phys. Lett.* **89**, 222512 (2006).
- ⁶V. Franco, A. Conde, V. K. Pecharsky, and K. A. Gschneidner, Jr., *Europhys. Lett.* **79**, 47009 (2007).
- ⁷M. D. Kuzmin, M. Richter, and A. M. Tishin, *J. Magn. Magn. Mater.* **321**, L1 (2009).
- ⁸V. Franco and A. Conde, *Int. J. Refrigeration* **33**, 465 (2010).
- ⁹J. Lyubina, M. D. Kuzmin, K. Nenkov, O. Gutfleisch, M. Richter, D. L. Schigel, T. A. Lograsso, and K. A. Gschneidner, Jr., *Phys. Rev. B* **83**, 012403 (2011).
- ¹⁰M. D. Kuzmin, K. P. Skokov, D. Y. Karpenkov, J. D. Moore, M. Richter, and O. Gutfleisch, *Appl. Phys. Lett.* **99**, 012501 (2011).
- ¹¹A. Biswas, S. Chandra, T. Samanta, M. H. Phan, I. Das, and H. Srikanth, *J. Appl. Phys.* **113**, 17A902 (2013).
- ¹²A. Biswas, S. Chandra, T. Samanta, B. Ghosh, S. Datta, M. H. Phan, A. K. Raychaudhuri, I. Das, and H. Srikanth, *Phys. Rev. B* **87**, 134420 (2013).
- ¹³P. Lampen, N. S. Bingham, M. H. Phan, H. Kim, M. Osofsky, A. Piqué, T. L. Phan, S. C. Yu, and H. Srikanth, *Appl. Phys. Lett.* **102**, 062414 (2013).
- ¹⁴T. Krenke, E. Dumn, M. Acet, E. Wassermann, X. Moya, L. Manosa, and A. Planes, *Nature Mater.* **4**, 450 (2005).
- ¹⁵V. K. Sharma, M. K. Chattopadhyay, R. Kumar, T. Ganguli, P. Tiwari, and S. B. Roy, *J. Phys.: Condens. Matter* **19**, 496207 (2007).
- ¹⁶Z. D. Han, D. H. Wang, C. L. Zhang, H. C. Xuan, B. X. Gu, and Y. W. Du, *Appl. Phys. Lett.* **90**, 042507 (2007).
- ¹⁷T. L. Phan, P. Zhang, N. H. Dan, N. H. Yen, P. T. Thanh, T. D. Thanh, M. H. Phan, and S. C. Yu, *Appl. Phys. Lett.* **101**, 212403 (2012).
- ¹⁸C. Marcela Bonilla, J. Herrero-Albillos, F. Bartolome, L. M. Garcia, M. Parra-Borderias, and V. Franco, *Phys. Rev. B* **81**, 224424 (2010).
- ¹⁹M. H. Phan and S. C. Yu, *J. Magn. Magn. Mater.* **308**, 325 (2007).
- ²⁰T. Samanta, I. Das, and S. Banerjee, *J. Appl. Phys.* **104**, 123901 (2008).